

1 **Investigation of morphological and mechanical properties of**
2 **hardened and tempered AISI 4340 steel**

3 SUBHAN ALI^{1*}, ABDUL QADEER LAGHARI^{2**}, ARSHAD IQBAL³, GHULAM
4 MUSTAFA MEMON⁴, IFITKHAR AHMED MEMON¹, FIDA HUSSAIN CHANNA⁵,
5 ABDUL SAMI CHANNA⁶, MASROOR ABRO², KHAN MUHAMMAD³
6 and SHOUKAT ALI NOONARI⁷

7 ¹Materials Engineering Department, Dawood University of Engineering and Technology,
8 Karachi, 74800, Sindh, Pakistan, ²Chemical Engineering Department, Mehran University of
9 Engineering and Technology, Jamshoro, 76080, Pakistan, ³Chemical Engineering
10 Department, Dawood University of Engineering and Technology, Karachi, 74800, Sindh,
11 Pakistan, ⁴IRC for Industrial Nuclear Energy, King Fahd University of Petroleum &
12 Minerals, Saudi Arabia, ⁵Mining Engineering Department, Mehran University of Engineering
13 and Technology, Jamshoro, 76080, Pakistan, ⁶Chemical Engineering Department,
14 Qaid-e-Awam University of Engineering and Technology, Nawabshah, 74800, Pakistan and
15 ⁷Department of Mechanical Engineering, Isra University, Hyderabad, Sindh, Pakistan

16 (Received 23 November, revised 26 December 2025, accepted 9 March 2026)

17 *Abstract:* AISI 4340 steel is widely used in risk-intensive industries due to its
18 excellent mechanical strength and impact resistance. The mechanical properties
19 of AISI 4340 steel can be significantly enhanced through heat treatment, par-
20 ticularly tempering at controlled temperatures. This study investigates the effect
21 of tempering on the microstructure and mechanical properties of AISI 4340 steel.
22 The experimental analysis includes characterization before and after heat treatment
23 to assess changes in strength, toughness and ductility. The results demonstrate
24 that tempering at 450 °C for 45 min provides the optimum balance of impact
25 energy and ductility while slightly reducing hardness and strength. Conversely,
26 tempering at 550 °C results in a more pronounced increase in impact energy and
27 ductility, but at the cost of a greater reduction in hardness and strength. Micro-
28 structural examination confirms the formation of tempered martensite, contri-
29 buting to the observed mechanical behaviour. The findings provide valuable
30 insights into optimizing heat treatment parameters for AISI 4340 steel to achieve
31 a balanced combination of strength, toughness, and ductility for industrial applic-
32 ations.

33 *Keywords:* AISI 4340 steel; tempering; mechanical properties; heat treatment.

*,** Corresponding authors. E-mail: (*)subhan.jogi@duet.edu.pk,
(**)abdul.qadeer@admin.muet.edu.pk
<https://doi.org/10.2298/JSC251123012A>

INTRODUCTION

34
35
36
37
38
39
40
41
42
43
44
45
46
47
48
49
50
51
52
53
54
55
56
57
58
59
60
61
62
63
64
65
66
67
68
69
70
71
72
73

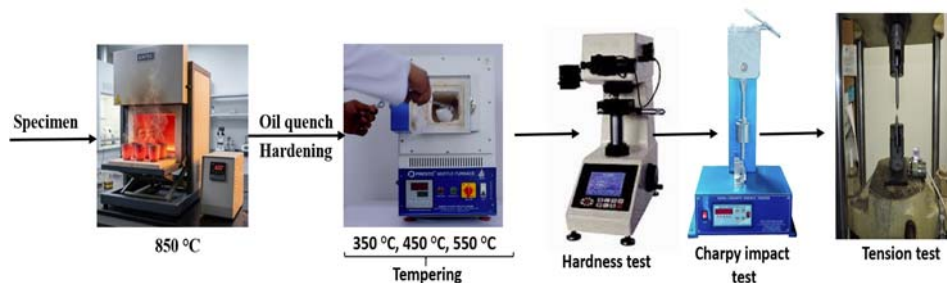
Low alloy AISI 4340 steel has found application in the military sector, critical aircraft components, and nuclear power plants, attributable to its mechanical properties such as tensile strength, stiffness, exceptional processability, optimal hardness and improved weldment.^{1,2} Nickel in steel, compared to that in other medium and low alloy steels, enhances tensile toughness and hardness.³ It has been reported that high-strength steels used in industries suffer from unexpected brittle failure.⁴ The catastrophic failure of engineering components under service conditions, shutdown of power plants, and elevated impairment costs of engineering machine components are serious consequences during operation.^{5,6} Dual-phase steel structures produced by various means have been planned nowadays for the proud performance of structural steel.⁷ Reported work clarified the effect of quenching and tempering treatments for optimising properties of AISI 4340 steel.⁸ Additionally, quenching and tempering treatments significantly increase the ultimate tensile strength of the steel.⁹ Published work rectified that quenching and tempering heat treatment can be used to develop the tempered martensitic steel.¹⁰ Moreover, the hardening treatment of AISI 4340 steel substantially increases the toughness and minimised brittle fracture.^{11,12} Furthermore, recommendations regarding the toughness and strength of AISI 4340 steel indicate that the heat treatments for homogenization, normalizing, quenching and tempering, inter-critical annealing, austempering and martempering may be required.¹³ Subsequently, it was demanded that the upgrading of mechanical properties of AISI 4340 steel by numerous heat treatments procedures and by controlled metal-forming processes.¹⁴ Likewise, an inter-critical quenching process was applied to produce austenite phase for TRIP steel.¹⁵ Nevertheless, difficulties in metal forming processes and high operating equipment costs in process industries. In alternative, it was conveyed that a substantial alteration in the mechanical properties of steel is achieved by intermediate quenching treatment.¹⁶ For the advancement of AISI 4340 steel is used in quench and temper form, though, it is susceptible to embrittlement when tempered at temperatures ranging from 300 to 400 °C.¹⁷ The embrittlement problems addressed by many researchers in their findings that changes in micrographs and mechanical properties at diverse tempering temperatures.¹⁸ Temper heat treatment can be used as a stress relief procedure, confirming reduction of tensile residual stresses, which have badly influence on fatigue life of components.¹⁹ Despite widespread usage in industries of AISI 4340 steel and detailed study of the mechanical performance of the material, there is little published work in literature about the effect of heat treatment parameters on residual stresses.²⁰ The objective of the present work is to optimise mechanical properties of steel AISI 4340 through hardening treatment. The hardening method improves the strength and stiffness of materials by treating them at a specified temperature followed by quenching in water and oil medium.²¹

74 Temper treatment practice in ferrous materials is useful after hardening.²² In tem-
 75 pering procedure, steel is subjected to heating and cooling below the transfor-
 76 mation temperature range and takes time for cooling at a suitable rate.²³ Tempering
 77 treatment causes of reduction in hardness and increases the toughness to get the
 78 desired mechanical properties.^{24,25} Hence, in current study, AISI 4340 high
 79 strength low alloy steel has been designated and treated at suitable temperature to
 80 stabilize the microstructure for optimisation of mechanical properties. AISI 4340
 81 steel applied in machine components, but it is required for service conditions in
 82 various forms extending from aircraft structures to automotive crankshafts, where
 83 diverse characteristics are required.²⁶ In this study, hardening and tempering
 84 techniques are employed to alter the mechanical properties and microstructure of
 85 AISI 4340 high strength low alloy steel through heat treatment. In addition, out-
 86 comes of this research were compared with conventional hardening and tempering
 87 of steel. Conclusively, the optimal conditions for attaining the highest toughness
 88 were achieved.

89 EXPERIMENTAL PROCEDURE

90 *Material*

91 Work material for the heat-treatment procedure was made by partitioning AISI 4340 steel
 92 bar into cross-sectional areas of 0.621 m² and 0.914 m length. The material in the form of a
 93 billet is rolled into a round bar and then cooled in air during the manufacturing procedure of
 94 AISI 4340 steel in an industrial unit (Fig. 1).



95
96 Fig. 1. Experimental setup of AISI 4340 steel bar.

97 *Chemical configuration*

98 The surface of the specimen was prepared by grinding followed by polishing to eliminate
 99 surface particles and additional contamination. An optical emission spark spectrometer was
 100 used to determine the chemical elements present in the samples. Argon gas was used as an inert
 101 atmosphere gas medium through a purifier in the spectrometer. After argon gas stabilization,
 102 the specimen was positioned on an anvil and clamped.²⁷ A minimum of three sparks per speci-
 103 men were made on different positions of the polished surface to determine the average values
 104 and standard deviation. Percentage of the elements present in AISI 4340 steel at the initial stage
 105 of the study is discussed in Table I.²⁸

106 TABLE I. Chemical analysis of AISI 4340 steel before heat treatment

Element	C	Si	Mn	Cr	Mo	Ni	T	Cu	Co	P	S	Fe
wt. %	0.37	0.25	0.70	0.82	0.02	0.11	0.14	0.15	0.006	0.016	0.019	Balance

107 *Heat treatment procedure*

108 The standard specimens for the impact and tensile tests were prepared from the round bars
109 of AISI 4340 steel placed in a muffle furnace for hardening at 850 °C for 45 min, followed by
110 oil quenching in mineral oil. The hardened heat-treated work material was tempered at 350, 450
111 and 550 °C and allowed to cool to room temperature.

112 *Hardness testing trials*

113 Hardened and tempered samples were investigated by using a Vickers hardness testing
114 machine HM-100 Series (HV-100), Japan, to measure the resistance to indentation.²⁹ Indenta-
115 tion was made on well-prepared specimens. A 20 kg load was applied for indentation, and the
116 indentations were examined using a microscope. Indentation was measured at an appropriate
117 distance from the sample edge to avoid any edge effects. Three different measurements were
118 made to identify the hardness value of the standard specimen.

119 *Charpy impact testing technique*

120 Impact testing for energy absorption of heat-treated samples was conducted by applying
121 the force of a swinging pendulum. The geometry of the specimens for the Charpy impact test
122 was in accordance with ASTM standard E23 using a Charpy impact testing machine XJJD-50
123 China.³⁰ The specimens were prepared according to ASTM standard E23.

124 *Tension testing*

125 In the tension test, standard samples were fixed in the grips of the tensile testing machine
126 (ZwickRoell SE-250KN, ZwickRoell Group, Germany) equipped with an electronic load cell.
127 The upper crosshead of the tension testing machine dragged the specimens upward to failure
128 with a constant crosshead speed of 10 mm s⁻¹, to maintain a preliminary strain rate of 2.8 × 10⁻⁴.
129 The stress-strain diagram showed the mechanical properties such as yield strength, ultimate
130 tensile strength and toughness before fracture. The dimension of tensile test samples were in
131 accordance with ASTM standard E8.³¹

132 RESULTS AND DISCUSSION

133 *AISI 4340 steel in the as-received condition*

134 At first, the chemistry of AISI 4340 steel was analysed and given in Table II.
135 In the chemical analysis, it was evident that 0.82 % Cr is an alloying element
136 present in the steel to enhance resistance against degradation. The strength, tough-
137 ness, hardness (30 kg load), energy absorption, and tensile properties of the initial
138 samples are presented in Table II.

139 TABLE II. Mechanical properties of the work material before treatment

Material	HVN (30 kg)	Impact <i>E</i> J	UTS MPa	Breaking stress MPa	Elongation %
AISI 4340 before treatment	135	9.5	715	468.73	33.92

140 Pictorial views of as-received samples of AISI 4340 steel confirm the iden-
 141 tification of ferrite structure and pearlite phase in microstructural examination, and
 142 the lighter phase corresponds to ferrite. Micrographs were recorded *via* a light
 143 optical microscope.

144 *Heat treatment*

145 This contemporary study is capable of enhancing the energy absorption and
 146 strength of AISI 4340 low-strength high-alloy steel *via* heat treatment pro-
 147 cesses; consequently, once the work pieces were ready for mechanical characteriz-
 148 ation. At the beginning selected samples were subjected to hardening at 850 °C for
 149 45 min and followed by quenching. Secondly, the specimens were tempered at
 150 350, 450 and 550 °C for 45 min and quenched in air.^{32,33}

151 *Hardening procedure of AISI 4340 steel*

152 Following the hardening heat treatment of AISI 4340 steel, it was found that
 153 Vickers hardness values increased considerably to 625 (30 kg), whereas the absor-
 154 bed energy and internal reactive force decreased to 7.53 J and 1520 MPa, res-
 155 pectively. The hardening of AISI 4340 steel reduced the ductility and increased the
 156 brittleness. The micrograph contains very fine-grained martensitic regions. Since
 157 martensitic regions have a BCT crystal structure and are considered as the hardest
 158 phase.³⁴ The pictorial views of the hardening treatment have good agreement with
 159 the outcomes reported previously.

160 *Tempering technique of AISI 4340 steel*

161 Tempering treatment after the hardening procedure improves the strength and
 162 ductility of the martensitic phase structure of AISI 4340 steel, whereas decreases
 163 the hardness.³⁵ Findings of tempering heat treatment are arranged in tabular form
 164 Table III. Statistical analysis of the mechanical properties of the materials (AISI
 165 4340 steel) is presented in the comparative graph shown in Fig. 2.

166 TABLE III. Mechanical properties of the work material after temper treatment

Material	Tempering temp., °C	HVN (30 kg)	Impact <i>E</i> J	UTS MPa	Elongation %
AISI4340	350	232.6	10.49	1400.69	22.59
	450	219	20	1456.98	29.32
	550	198.13	39	1255.07	30.99

167 It was discovered that the toughness and hardness of the work material are
 168 affected by heating in a furnace for hardening and followed by tempering at
 169 different temperature levels. Hardening treatment achieved the utmost hardness
 170 and tensile strength and reduced the percentage elongation.³⁶ As reported by
 171 researchers, the phase change of AISI 4340 steel might be due to the quenching

172 route, where abrupt changes occur in crystal structure phase from gamma (γ), *i.e.*,
 173 FCC to BCT and a martensitic phase structure.³⁷ Rapid intensification in Vickers
 174 hardness and strengths occurs during transformation in platelets of the martensite
 175 phase, producing enormous alteration, and the same trend was also observed on
 176 similar materials.³⁸ It can be seen from the tempering results that improvement of
 177 hardness, ultimate strength and toughness is shown in Fig. 2.

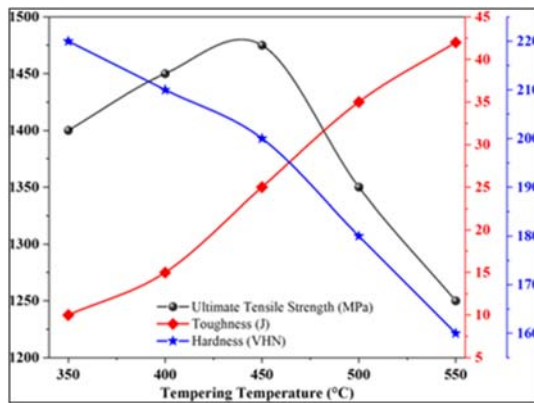


Fig. 2. Comparative analysis of mechanical properties after tempering of hardened AISI 4340 steel at 350–550 °C for 45 min.

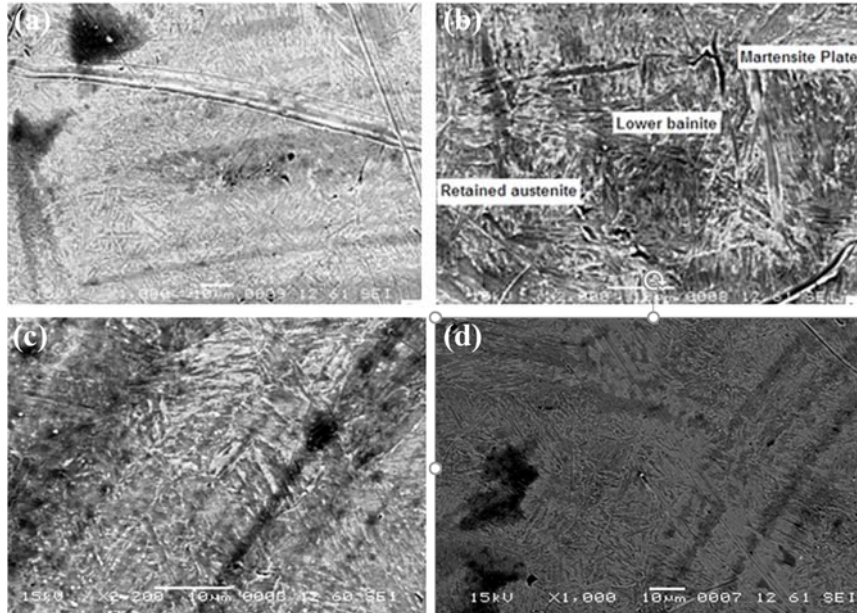
178 The comparative analysis of the heat-treatment results showed that hardness
 179 and strength were drastically reduced from 625 to 232.6 *HVN* at 30 kg, and from
 180 1520 to 1400.69 MPa, respectively, whereas the energy absorption increased from
 181 7.53 to 10.49 J. Based on the results, it can be concluded that internal stresses
 182 produced by changes in martensitic morphology and contributed to improved duct-
 183 ility. Moreover, a notable change in mechanical properties of the AISI4340 steel
 184 was obtained after tempering at 450 °C for 45 min. Furthermore, analysis of the
 185 data after heat treatment of AISI 4340 steel showed a decline in hardness values
 186 and an increase in strengths and toughness. This can be attributed to the fact that
 187 the section was tempered at 550 °C for the same duration, resulting in a decrease
 188 in hardness and tensile strength but an increase in toughness. Hence, tempering
 189 heat treatment practice of AISI 4340 steel at 450 °C achieves an optimum balance
 190 of hardness, tensile strength and toughness.¹³ Experimental evidence shows that
 191 low-carbon Mn–Si–Cr steel, when quenched after the hardening procedure, causes
 192 phase conversion and affects the mechanical properties.

193 *Scanning electron microscopy analysis*

194 High-strength low-alloy steel is designed particularly for space shuttle,
 195 aircraft, and missile structures for defence applications. AISI 4340 steel was sub-
 196 jected to heating and cooling processes to improve fracture resistance and enhance
 197 tensile strengths. By heat treatment, the mechanical strength properties of high

198 strength low alloy steel were modified through tempering and subsequent quen-
199 ching.³⁹ Phase change of steel occurs by the hardening and tempering technique.
200 The transformed microstructures, like retained austenite, lower bainite, martensite
201 and some carbides, were recognized by means of a high-resolution transmission
202 electron microscope.⁴⁰ It can also be discussed that retained austenite is capable of
203 arresting crack propagation and increases resistance to fracture of low alloy
204 medium carbon steel. Furthermore, research findings indicate that the cracks trav-
205 eling through martensite are impassable while passing through a region of retained
206 austenite. If internal reactive forces are present, cracks harvest the branches and
207 started to increase close to austenite region, therefore more energy is absorbed
208 through the martensite plates and this promotes the toughness of steel. AISI 4340
209 steel containing lower bainite and tempered martensite as a dual phase is exten-
210 sively studied concerning its mechanical properties. It is notified that the dual-
211 -phase steel provides a healthier combination of strength and toughness compared
212 with wholly martensitic structures.⁴¹ discussed previously from the optical micro-
213 graphs, detailed information regarding variations occurring through the phase alt-
214 eration process was required, hence, it was found essential to inspect hardened and
215 tempered work pieces by using SEM. The micrograph in Fig. 3a shows evidence
216 of a dual-phase microstructure containing lower bainite and martensitic structure
217 of AISI 4340 steel tempered at a temperature of 350 °C for 45 min. The SEM
218 microstructure captured at high resolution and magnification is displayed in Fig.
219 3b, showing a dual-phase microstructure of lower bainite and martensite plates
220 layered with an austenitic phase structure on the grain boundaries. A comparable
221 topography was detected (Fig. 3c and d), for the specimens inspected with high
222 resolution SEM after tempering at 450 and 550 °C for 45 min.

223 In this contemporary study, a steel grade was hardened and tempered to reduce
224 the hardness associated with martensitic structure while enhancing the high-energy
225 region. It has been testified by numerous investigators.⁴² that P, S and Sn and
226 antimony have an adverse effect on steel showing a brittle appearance once tem-
227 pered. Impurities present in the steel tend to segregate near the austenitic region
228 and decohesion across the grain boundaries, which eventually results in inter gra-
229 nular brittle failure. These consequences arise from impurity segregation promoted
230 by tempering treatment of steel at elevated temperature. While the similar steel
231 grade, when quenched from elevated temperature, irregularities within the material
232 do not activate during cooling and therefore reduce the embrittlement mechanism
233 of fracture. As is evident from reported results, tempered specimens failed during
234 tensile test and were studied using a scanning electron microscope. The micro-
235 graph shown in Fig. 4a represents the fractured surface of a work piece tempered
236 at 350 °C, scrutinized under a scanning electronic microscope and conforming
237 stress-strain photograph. AISI 4340 sectioned pieces exhibited intergranular frac-
238 ture, which is characteristic of brittle fracture. Illustration of stress-strain diagram

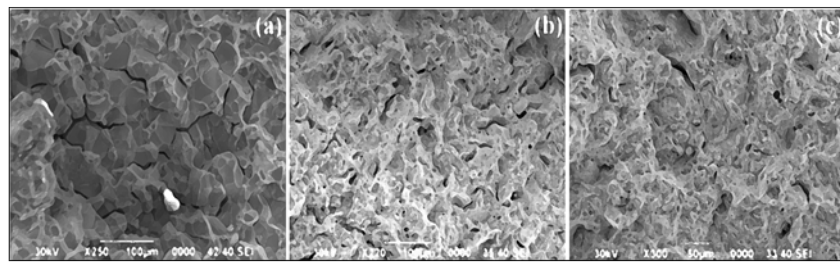


239
240
241

Fig. 3. SEM micrograph of AISI 4340 steel tempered at: a) 350 and b) 450 °C; comparative topography at: c) 450 and d) 550 °C.

242 did not present any yielding and elongation all through the tensile test. These
243 values indicate brittle fracture material behaviour. Fracture along the grain bound-
244 aries of the tempered martensitic phase structure is in good agreement with dis-
245 coveries conferred previously. New findings quantified in Table IV signify the
246 tempering temperature at 350 °C. The hardness values are comparatively higher
247 and impact energy is relatively lower than the finding of hardness and impact
248 energy noted when tempered at 450 °C. Illustration of Table IV also indicates an
249 increase in tensile strength of the work material. Therefore, the increase in impact
250 energy is accompanied by considerable reduction in the hardness and strength of
251 the specimens.⁴³ Micrographs were recorded for AISI 4340 steel tempered at 350,
252 450 and 550 °C, as presented in Fig. 4a–c. As the tempering temperature increases,
253 the fracture morphology exhibits a distinct change in failure mode, which is direct-
254 ly correlated with modifications in mechanical behaviour. The fracture surface
255 primarily displays intergranular and quasi-cleavage features in Fig. 4a, which cor-
256 responds to tempering at 350 °C. This suggests a relatively brittle fracture mech-
257 anism. Tempered martensite with high residual stresses and fine ϵ -carbides, which
258 restrict plastic deformation and encourage crack initiation along previous austenite
259 grain boundaries, is linked to this behaviour. As a result, this condition is usually
260 characterized by increased strength and hardness but reduces toughness. As seen
261 in Fig. 4b, the fracture mode changes towards ductile fracture when the tempering
262 temperature is raised to 450 °C. Microvoid nucleation, growth and coalescence

263 produce uniformly distributed dimples on the fracture surface. This transition
 264 shows increased plasticity as a result of controlled cementite (Fe_3C) precipitation
 265 and partial martensitic structure recovery. Strength and toughness are better bal-
 266 anced at this tempering condition, which is frequently regarded as ideal for AISI
 267 4340 steel. The fracture surface exhibits deeper and larger dimples at the maximum
 268 tempering temperature of 550 °C (Fig. 4c), indicating a fully ductile fracture
 269 mechanism. Carbide coarsening and spheroidisation, as well as substantial stress
 270 relief and martensite breakdown into a ferrite-carbide matrix are responsible for
 271 the increase in dimple size. This microstructural evolution leads to increased duct-
 272 ility and impact toughness but decreased hardness and strength. The evolution of
 273 carbide precipitation Fe_3C and the transformation of the martensitic phase are
 274 reflected in the progressive increase in dimple size with tempering temperature.
 275 The observed trends in the mechanical properties of tempered and hardened AISI
 276 4340 steel are strongly supported by these morphological changes seen in SEM
 277 fractography.



278
 279 Fig. 4. SEM Analysis of samples after tempering at: a) 350, b) 450 and c) 550 °C.

280 TABLE IV. Tensile properties of AISI 4340 steel at various tempering temperatures

Sample	Tempering temp., °C	Diameter (d_0 / mm)	L_0 / mm	F_{max} N/mm ²	F_{Break} %	e_{Break} %	$e-F_{max}$ %
(a)	350	12.5	35.08	1400.09	1400.09	22.59	22.59
(b)	450	12.5	35.14	1456.96	1186.72	36.53	29.32
(c)	550	12.5	30.07	1255.02	980.52	41.47	30.99

281 Table IV presents the tensile properties of three samples subjected to different
 282 tempering temperatures (350, 450 and 550 °C), has been fixed by chamber oven
 283 UF160-Memmert GmbH+Co. Kg, Germany, highlighting the influence of heat
 284 treatment on tensile behaviour. At 350 °C, the sample exhibits a maximum stress
 285 of 1400.09 N/mm², Fig. 5, which increases to 1456.96 N/mm² at 450 °C, indicating
 286 enhanced strength due to the tempering-induced microstructural changes, such as
 287 stress relief and carbide precipitation. However, a further increase in tempering
 288 temperature to 550 °C results in a reduction to 1255.02 N/mm², suggesting over-
 289 tempering, where coarsening of the microstructure and reduction in dislocation

290 density lead to decreased strength. A similar trend is observed in the fracture
 291 strength, which drops significantly from 1400.09 % at 350 °C to 980.52 % at
 292 550 °C, reflecting a loss in the material's ability to withstand stress before failure
 293 as it becomes more ductile. Meanwhile, the elongation at break (e_{Break}) and at
 294 maximum stress ($e-F_{max}$) increase progressively with tempering temperature,
 295 rising from 22.59 % at 350 °C to 41.47 and 30.99 %, respectively, at 550 °C. This
 296 indicates a clear enhancement in ductility due to the transformation of the brittle
 297 martensitic structure into a more plastic and deformable phase. The results reveal
 298 a classic trade-off between strength and ductility with increasing tempering tem-
 299 perature. The sample tempered at 450 °C demonstrates an optimal combination of
 300 high tensile strength and improved elongation, suggesting that it may offer the best
 301 mechanical performance among the three conditions for applications requiring
 302 both durability and formability.

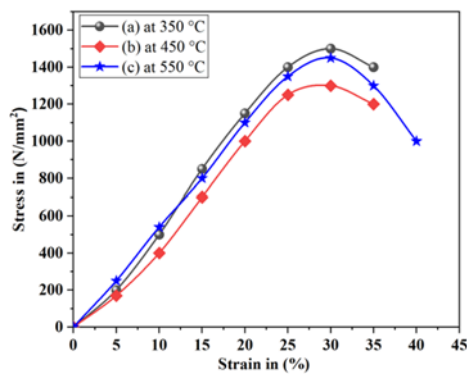


Fig. 5. Illustration of the tensile properties of AISI 4340 steel at different tempering temperatures.

303

CONCLUSION

304 This study investigated the tempering of AISI 4340 steel to optimize its mech-
 305 anical properties, finding that different tempering temperatures yield distinct results.
 306 Tempering at 350 °C primarily enhances tensile strength without significantly
 307 improving ductility or impact energy, while a higher temperature of 450 °C for 45
 308 min provides an optimal balance, effectively increasing both toughness and ductility
 309 while maintaining acceptable levels of strength and hardness. Conversely, tempering
 310 at 550 °C leads to a further increase in impact energy and ductility but results in a
 311 more significant reduction in strength and hardness. This observed behaviour is direct-
 312 ly linked to the formation of tempered martensite within the steel's microstruc-
 313 ture, as confirmed by microstructural analysis. Therefore, the findings suggest that a
 314 tempering treatment of 450 °C for 45 min is the most effective approach for
 315 achieving a desirable combination of mechanical properties for a wide range of eng-
 316 ineering applications.

- 361 8. R. Seede, B. Zhang, A. Whitt, S. Picak, S. Gibbons, P. Flater, A. Elwany, R. Arroyave, I.
362 Karaman, *Addit. Manuf.* **47** (2021) 102255
363 (<https://doi.org/10.1016/j.addma.2021.102255>)
- 364 9. Y. Zhang, J. Yang, D. Xiao, D. Luo, C. Tuo, H. Wu, *Metals* **12** (2022) 1087
365 (<https://doi.org/10.3390/met12071087>)
- 366 10. F. Deirmina, N. Peghini, B. AlMangour, D. Grzesiak, M. Pellizzari, *Mater. Sci. Eng., A*
367 **753** (2019) 109 (<https://doi.org/10.1016/j.msea.2019.03.027>)
- 368 11. F. Hosseinifar, A. Ekrami, *Mater. Sci. Eng., A* **830** (2022) 142314
369 (<https://doi.org/10.1016/j.msea.2021.142314>)
- 370 12. A. Khodabandeh, D. Sayadi, S. Rajabi, M. Khosrojerdi, M. Khajehzadeh, M. R. Razfar,
371 *Proc. Inst. Mech. Eng., C.: J. Mech. Eng. Sci.* **238** (2024) 7607
372 (<https://doi.org/10.1177/09544062241232236>)
- 373 13. M. Parvinzadeh, S. S. Karganroudi, N. Omid, N. Barka, M. Kh Int. *J. Adv. Manuf.*
374 *Technol.* **115** (2021) 1 (<https://doi.org/10.1007/s00170-021-07351-5>)
- 375 14. M. K. Sanij, S. G. Banadkouki, A. Mashreghi, M. Moshrefifar, *Mater. Des.* **42** (2012) 339
376 (<https://doi.org/10.1016/j.matdes.2012.06.017>)
- 377 15. A. Kokosza, J. Pacyna, *Arch. Metall. Mater.* **59** (2014) 1017
378 (<https://doi.org/10.2478/amm-2014-0170>)
- 379 16. I. Dey, R. Saha, B. Mahato, M. Ghosh, S. Ghosh, *Metall. Mater. Trans., A* **55** (2024) 1
380 (<https://doi.org/10.1007/s11661-024-07431-7>)
- 381 17. M. de Souza, L. F. Serrão, J. M. Pardal, S. S. M. Tavares, M. C. Fonseca, *Int. J. Adv.*
382 *Manuf. Technol.* **120** (2021) 1123 (<https://doi.org/10.1007/s00170-022-08880-3>)
- 383 18. S. Sharma, J. Singh, M. K. Gupta, M. Mia, S. P. Dwivedi, A. Saxena, S. Chattopadhyaya,
384 R. Singh, D. Y. Pimenov, M. E. Korkmaz, *J. Mater. Res. Technol.* **12** (2021) 1564
385 (<https://doi.org/10.1016/j.jmrt.2021.03.095>)
- 386 19. M. Kumaran, S. Ravi, *Mater. Lett.* **377** (2024) 137427
387 (<https://doi.org/10.1016/j.matlet.2024.137427>)
- 388 20. D. Schröpfer, A. Kromm, T. Lausch, M. Rhode, R. Wimpory, T. Kannengießler, *Weld.*
389 *World.* **14** (2021) 1 (<https://doi.org/10.1007/s40194-021-01101-7>)
- 390 21. J. Yang, Z. Zhu, S. Han, Y. Gu, Z. Zhu, H. Zhang, *J. Alloys Compd.* **1008** (2024) 176707
391 (<https://doi.org/10.1016/j.jallcom.2024.176707>)
- 392 22. T. Sonar, S. Lomte, C. Gogte, *Mater. Today: Proc.* **5** (2018) 25219
393 (<https://doi.org/10.1016/j.matpr.2018.10.324>)
- 394 23. V. S. J. Milton, Z. C. J. Wilmer, H. A. D. Bryan, Z. C. J. Gregorio, Á. R. A. Linzan, M.
395 E. C. Guaigua, A. C. Z. Rodríguez, *Nanotechnol. Perceptions* **20** (2024) 307
396 (<https://doi.org/10.62441/nano-ntp.vi.408>)
- 397 24. E. Tkachev, S. Borisov, A. Belyakov, T. Kniaziuk, O. Vagina, S. Gaidar, R. Kaibyshev,
398 *Mater. Sci. Eng., A* **868** (2023) 144757 (<https://doi.org/10.1016/j.msea.2023.144757>)
- 399 25. A. Panda, R. Bag, A. K. Sahoo, R. Kumar, *Int. J. Integr. Eng.* **12** (2020) 61
400 (<https://publisher.uthm.edu.my/ojs/index.php/ijie/article/view/5667>)
- 401 26. A. Saboori, A. Aversa, G. Marchese, S. Biamino, M. Lombardi, P. Fino, *Appl. Sci.* **9**
402 (2019) 3316 (<https://doi.org/10.3390/app9163316>)
- 403 27. J. Miao, L.-l. Yu, X.-g. Liu, B.-f. Guo, *Trans. Nonferrous Met. Soc. China* **28** (2018)
404 2082 ([https://doi.org/10.1016/S1003-6326\(18\)64852-6](https://doi.org/10.1016/S1003-6326(18)64852-6))

- 405 28. J. Yan, C. Zhang, J. Guo, G. Dong, S. Wang, J. Gao, H. Wu, H. Zhao, J. Lu, Y. Huang,
406 X. Mao, *J. Mater. Res. Technol.* **38** (2025) 3264
407 (<https://doi.org/10.1016/j.jmrt.2025.08.142>)
- 408 29. M. A. Hafeez, M. Usman, M. A. Arshad, M. AdeelUmer, *Crystals* **10** (2020) 508
409 (<https://doi.org/10.3390/cryst10060508>)
- 410 30. L. F. Monaheng, W. B. du Preez, C. Polese, *Metals* **11** (2021) 1736
411 (<https://doi.org/10.3390/met11111736>)
- 412 31. J. Na, J. Middendorf, M. Lander, J. Waller, R. Rauser, in *Structural Integrity of Additive*
413 *Manufactured Parts*, N. Shamsaei, S. Daniewicz, N. Hrabe, S. Beretta, J. Waller, M.
414 Seifi, Eds., ASTM International, West Conshohocken, PN, 2020, p. 206
415 (<https://doi.org/10.1520/STP162020180095>)
- 416 32. S. Bakhshi, M. Asadi Asadabad, S. Bakhshi, S. Bakhshi, *Ironmak. Steelmak.* **50** (2023)
417 295 (<https://doi.org/10.1080/03019233.2022.2107111>)
- 418 33. S. Khatai, A. K. Sahoo, R. Kumar, A. Panda, *Proc. Inst. Mech. Eng., C: J. Mech. Eng.*
419 *Sci.* **238** (2024) 10997 (<https://doi.org/10.1177/09544062241276347>)
- 420 34. W. Tan, , *PhD Thesis*, New York State College of Ceramics at Alfred University, 2017,
421 (<http://hdl.handle.net/10829/24629>)
- 422 35. M. M. Bilal, K. Yaqoob, M. H. Zahid, W. H. Tanveer, A. Wadood, B. Ahmed, *J. Mater.*
423 *Res. Technol.* **8** (2019) 5194 (<https://doi.org/10.1016/j.jmrt.2019.08.042>)
- 424 36. S. Sharma, A. Kini, G. Shankar, T. Rakesh, H. Raja, K. Chaitanya, M. Shettar, *J. Mech.*
425 *Eng. Sci.* **12** (2018) 3866 (<https://doi.org/10.15282/jmes.12.3.2018.8.0339>)
- 426 37. A. F. Brust, *PhD Thesis*, Ohio State University, 2019
427 (http://rave.ohiolink.edu/etdc/view?acc_num=osu1555523646156822)
- 428 38. M. Motyka, *Metals* **11** (2021) 481 (<https://doi.org/10.3390/met11030481>)
- 429 39. F. P. Li, N. Li, X. L. Wang, M. H. Liang, *Mater. Sci. Forum* **1035** (2021) 424
430 (<https://doi.org/10.4028/www.scientific.net/MSF.1035.424>)
- 431 40. X. Wang, C. Liu, Y. Qin, Y. Li, Z. Yang, X. Long, M. Wang, F. Zhang, *Mater. Sci. Eng.,*
432 *A* **832** (2022) 142357 (<https://doi.org/10.1016/j.msea.2021.142357>)
- 433 41. M. Elitas, *Mater. Test.* **63** (2021) 124 (<https://doi.org/10.1515/mt-2020-0019>)
- 434 42. G. Muthukumaran, P. D. Babu, *Arab. J. Sci. Eng.* **1008** (2022) 1
435 (<https://doi.org/10.1007/s13369-021-06350-8>)
- 436 43. F. A. Khatir, M. H. Sadeghi, S. Akar, *J. Manuf. Process.* **61** (2021) 173
437 (<https://doi.org/10.1016/j.jmapro.2020.09.073>).